International Journal of Solids and Structures 75–76 (2015) 188–198

Contents lists available at ScienceDirect

International Journal of Solids and Structures

journal homepage: www.elsevier.com/locate/ijsolstr

A piecewise exponential model for three-dimensional analysis of sandwich panels with arbitrarily graded core

B. Woodward, M. Kashtalyan *

Centre for Micro- and Nanomechanics (CEMINACS), School of Engineering, University of Aberdeen, Fraser Noble Building, Aberdeen AB24 3UE, UK

ARTICLE INFO

Article history:
Received 30 April 2015
Received in revised form 7 August 2015
Available online 27 September 2015

Keywords:
Three-dimensional elasticity
Analytical modelling
Finite element modelling

ABSTRACT

In this paper a piecewise exponential model is proposed for analysis of three-dimensional elastic deformation of rectangular sandwich panels with graded core subjected to transverse loading. The model can be applied to any functionally graded plate or sandwich panel with graded core as long as the through thickness stiffness variation can be described by a smooth function. The new piecewise exponential model is fully validated through both comparison with results from the literature and a three-dimensional finite element method which employs user-implemented graded finite elements. As an example the new model is applied to three dimensional elasticity analysis of sandwich panels with power law variation in stiffness properties of the core and a comparative study is carried out to examine the effect of panel thickness and varying the power law index on panel's response.

1. Introduction

Sandwich panels or plates are three layer structures comprising two face sheets of high strength and stiffness, separated by a core of lower density and strength. When combined, these layers provide sandwich panels with high specific strength and as such they are ideally suited to a variety of engineering applications, particularly in the aerospace industry. Due to the mismatch in stiffness properties between the face sheets and the core, sandwich panels are susceptible to delamination, caused by high interfacial stresses, especially under localised loading (Abrate, 1998) or at high service temperatures (Noda, 1999).

One effective method of minimising the large interfacial shear stresses is to make use of the functionally graded material concept for the panel core. Functionally graded materials are a type of heterogeneous composite materials exhibiting gradual variation in microstructure and composition of the two constituent materials from one surface of the material to the other, resulting in properties which vary continuously across the material. Comprehensive review of research on structures incorporating functionally graded materials is given by Birman and Byrd (2007), while more recent reviews (Liew et al., 2011; Jha et al., 2013; Swaminathana et al., 2015) focused specifically on functionally graded plates.

Sandwich panels with graded core have been studied analytically, numerically and experimentally by a number of researchers. Anderson (2003) developed a 3D elasticity solution for a sandwich panel with orthotropic face sheets and an isotropic functionally graded core subjected to transverse loading by a rigid sphere. Kirugulige et al. (2005) demonstrated feasibility of using functionally graded foam as core material in sandwich panels under impact loading conditions using graded core with a bilinear volume fraction variation. Zhu and Sankar (2007) studied sandwich panels with graded foam core used in thermal protection systems subjected to transverse loads. The Fourier analysis combined with the Galerkin method was used for solving the two-dimensional elasticity equations and analyse panels with arbitrary variation of thermo-mechanical properties in the thickness direction. The analysis was also performed using sandwich plate theory. Significant differences were found in the results suggesting that the sandwich theory may not be suitable for the analysis of thick sandwich panels. Apetre et al. (2008) investigated several available sandwich beam theories for their suitability to analysis of sandwich plates with functionally graded core. Kashtalyan and Menshykova (2009) developed a three dimensional elasticity solution for sandwich panels with functionally graded core whose shear moduli vary exponentially through the thickness of the core. Etemadi et al. (2009) performed a finite element analysis of low velocity impact behaviour of sandwich beams with a functionally graded core. Projectile velocity and beam geometry were varied and comparisons were made between a functionally graded and a homogeneous beam. The results showed that insertion of a graded core decreased the maximum strains, yet increased maximum contact force. Rahmani et al. (2009) analysed free vibrations of sandwich

* Corresponding author.
E-mail address: m.kashtalyan@abdn.ac.uk (M. Kashtalyan).

http://dx.doi.org/10.1016/j.ijsolstr.2015.08.012
0020-7683/

panels with graded syntactic core using a higher-order sandwich beam theory. Icardi and Ferrero (2009) carried out optimisation studies on sandwich panels to find the orientation of the reinforcement in the face sheets and the variation of the core properties across the thickness with the view to minimise the interlaminar stress concentration under point loading. They employed an approach based a refined zig-zag model with a high-order variation of displacements. Dynamic response of sandwich panels with E-glass/Vinyl Ester face sheets and graded styrene foam cores to shock wave loading was experimentally investigated by Wang et al. (2009). Woodward and Kashtalyan (2010, 2011, 2012) investigated three-dimensional elastic deformation of sandwich panels with exponentially graded core under a variety of loadings and boundary conditions using a combination of analytical and computational means. Circular sandwich panels with graded core were studied by Sburlati (2012). Exponential variation of Young's modulus through the core thickness was assumed to enable development of analytical solution to the axisymmetric problem. The low velocity impact response of sandwich structures based on layered cores has been studied both experimentally and numerically by Zhou et al. (2013). Thermo-elastic response and free vibrations of cylindrical sandwich panels with graded core were examined by Alibeigloo (2014) and Alibeigloo and Liew (2014). The dynamic responses and blast resistance of all-metallic sandwich plates with functionally graded close-celled aluminium foam cores were investigated using a finite element method and experimentally by Liu et al. (2014). Sandwich panels with lattice core graded in length direction were experimentally studied by Xu et al. (2015).

In the majority of analytical studies on sandwich panels with graded core either an exponential or power-law variation of stiffness properties through the thickness is assumed in order to enable development of the solution. However, there may be benefits in utilising cores with other variations in stiffness properties and so methods must be sought in order to model them. Extending existing methods and solutions to the case of arbitrary variation of stiffness seems to be a natural step in that direction.

In this paper, the three-dimensional elasticity solution for sandwich panels with exponential variation of the Young's modulus through the thickness (Kashtalyan and Menshykova, 2009) is extended to produce a piecewise exponential model that can be applied to any functionally graded plate or sandwich panel with graded core as long as the through thickness stiffness variation is described by a smooth function. Previously, approximation of arbitrary variation of material properties by a piecewise exponential model has been successfully applied to analysis of cracks in functionally graded materials (Guo and Noda, 2007; Bai et al., 2013), thermoelastic deformation of multilayered strips (Ootao, 2011) and plates (Ootao and Ishihara, 2013) and contact mechanics of graded coatings (Liu and Xing, 2014). To the best of our knowledge, this approach has not been applied yet to sandwich panels with graded core in the context of three-dimensional elasticity theory.

A piecewise-exponential model for sandwich panels with graded core presented in this paper is fully validated through both comparison with results from the literature and a finite element study. As an example the new model is applied to analysis of sandwich panels with power law variation in stiffness properties of the core and a study is carried out to examine the effect of varying the power law index on panel's response.

2. A piecewise-exponential model

A sandwich panel (Fig. 1) of length a, width b and total thickness $h_0 = 2h$ is referred to a Cartesian co-ordinate system $x_1, x_2, x_3 (0 \leqslant x_1 \leqslant a, 0 \leqslant x_2 \leqslant b, -h \leqslant x_3 \leqslant h)$ and assumed to be symmetric with respect to the mid-plane $x_3 = 0$, with the face

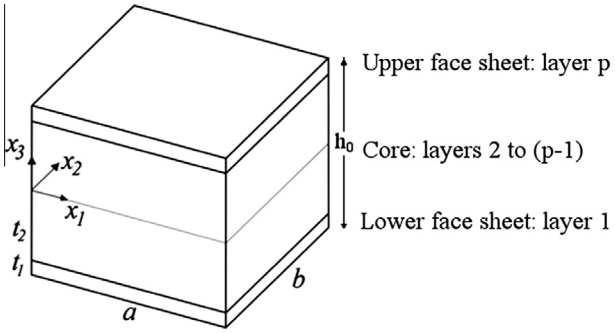

Fig. 1. Panel geometry.

sheet thickness h_f and the core thickness $2h_c$. The core of the panel is a functionally graded material, with the shear modulus that varies arbitrarily through the thickness, so that the actual shear modulus at any point is given by

$$G(x_3) = \Gamma(x_3) \tag{1}$$

where $\Gamma(x_3)$ is any smooth function. Poisson's ratios of the face sheets and the core are assumed to constant.

Referring to the idea of Guo and Noda (2007), let us divide the panel into p layers $(k = 1, 2 \ldots, p)$, with layers 1 & p being the face sheets and the core subdivided into p-2 layers. We assume that within each of the layers, actual variation of the shear modulus can be approximated by an appropriately chosen exponential function. Provided that a sufficiently high number of layers are used and that the actual material properties vary smoothly, then the continuously varying properties can be accurately simulated by the piecewise exponential model.

Let the shear modulus within each layer can be approximated by an exponential function

$$G^{(k)}(x_3) = g^{(k)} \exp\left\{\gamma^{(k)}\left(\frac{x_3}{h} - 1\right)\right\} \tag{2}$$

where $\gamma^{(k)}$ are the inhomogeneity parameters

$$\gamma^{(k)} = \frac{h}{t^{(k)}} \ln \delta^{(k)} \tag{3a}$$

and

$$\delta^{(k)} = \frac{G^{(k+1)}}{G^{(k)}}, \quad g^{(k)} = G^{(k)} \exp\left\{\gamma^{(k)}\left(1 - \frac{h^{(k)}}{h}\right)\right\} \tag{3b}$$

where $t^{(k)}$ is the thickness of the kth layer; $G^{(k)}$ and $G^{(k+1)}$ are the shear modulus values at the bottom of the kth and $(k+1)$th layers respectively; and $h^{(k)}$ is the height of the bottom of kth layer relative to the mid-plane. For ease of modelling, the homogenous face sheets $(k = 1,\ k = p)$ can also be treated as FGMs with the inhomogeneity parameters, $\gamma^{(k)}$, set sufficiently close to zero.

Using the actual material properties defined at each interface given by Eq. (1), expressions (3b) can be rewritten as follows

$$\delta^{(k)} = \frac{\Gamma(h^{(k+1)})}{\Gamma(h^{(k)})}, \quad g^{(k)} = \Gamma(h^{(k)}) \exp\left\{\gamma^{(k)}\left(1 - \frac{h^{(k)}}{h}\right)\right\} \tag{4}$$

Through the coefficients of the exponential functions, the number and thickness of the layers, many different variations in through thickness modulus can be modelled such as power law variation

$$\Gamma(x_3) = G_{tb}\left(\frac{|x_3|}{h_c}\right)^r + G_{core} \tag{5}$$

where $G_{tb} = G_{face} - G_{core}$, G_{face} is the shear modulus of the face sheets and G_{core} is the shear modulus at the centre of the core, and r is the power law index. A plot of through thickness variation of shear modulus in the sandwich panel for a range of values of r is given in Fig. 2. In order to approximate power law variation in shear moduli using the exponential function, the panel is split into 20 layers of equal thickness (layers 1 and 20 being the face sheets). The shear modulus is calculated at bottom, $G^{(k)}$, and top, $G^{(k+1)}$, of each layer using Eq. (5), and Eqs. (4a,b) and (3a) are then employed to calculate $\delta^{(k)}$, $g^{(k)}$ and $\gamma^{(k)}$ for each layer. Further discussion about the number of layers needed in the piecewise-exponential model is given in Section 4.

3. Solution of the three-dimensional elasticity problem

3.1. Boundary conditions

All layers are assumed to be perfectly bonded together, so that the continuity of stresses and displacements exists at all interfaces, i.e.

$$x_3 = x_3^{(k)} : \sigma_{i3}^{(k+1)} - \sigma_{i3}^{(k)} = 0, \quad u_i^{(k+1)} - u_i^{(k)} = 0, \quad i = 1,2,3 \tag{6}$$

where $\sigma_{ij}^{(k)}$ and $u_i^{(k)} (k = 1,\ldots,p-1)$ are the components of the stress tensor and displacement vector, respectively. The panel is subjected to transverse loading Q on the top surface, so that

$$x_3 = h : \sigma_{33}^{(p)} = Q(x_1,x_2), \quad \sigma_{13}^{(p)} = \sigma_{23}^{(p)} = 0. \tag{7a}$$

The loading $Q(x_1,x_2)$ is assumed to allow expansion into a Fourier series

$$Q(x_1,x_2) = -\sum_{m=1}^{\infty}\sum_{n=1}^{\infty} q_{mn} \sin\frac{\pi m x_1}{a} \sin\frac{\pi n x_2}{b} \tag{7b}$$

where q_{mn} is the intensity of the loading at the centre of the panel and m and n are wave numbers. The bottom surface of the panel is assumed to be load-free, i.e.

$$x_3 = 0 : \sigma_{33}^{(1)} = \sigma_{13}^{(1)} = \sigma_{23}^{(1)} = 0 \tag{8}$$

The Navier-type boundary conditions are assumed at the edges, so that

$$x_1 = 0, \quad a : \sigma_{11}^{(k)} = 0, \quad u_2^{(k)} = u_3^{(k)} = 0, \quad k = 1,\ldots,p \tag{9a}$$

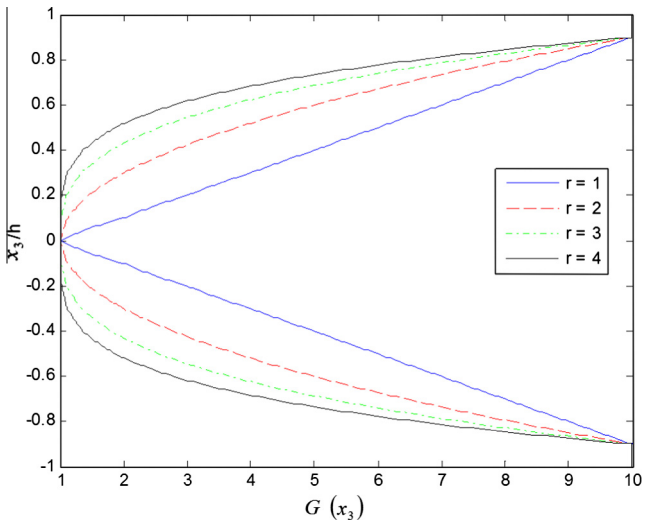

Fig. 2. Through-thickness variation of shear modulus in a sandwich panel for a range of power indices.

$$x_2 = 0, \quad b : \sigma_{22}^{(k)} = 0, \quad u_1^{(k)} = u_3^{(k)} = 0, \quad k = 1,\ldots,p \tag{9b}$$

The boundary conditions, Eq. (9), are representative of roller supports and analogous to simply supported edges in the plate theories (Kashtalyan, 2004).

3.2. Displacement functions method

To determine stresses and displacements in a p-layered sandwich panel subject to boundary conditions, Eqs. (6)–(9), Plevako's (1971) displacement functions $L^{(k)} = L^{(k)}(x_1,x_2,x_3)$ and $N^{(k)} = N^{(k)}(x_1,x_2,x_3)(k = 1,\ldots,p)$ are employed.

The displacements in the substrate and the coating can be expressed in terms of displacement functions as

$$u_1^{(k)} = -\frac{1}{2G^{(k)}}\left(\nu^{(k)}\Delta - \frac{\partial^2}{\partial x_3^2}\right)\frac{\partial L^{(k)}}{\partial x_1} + \frac{\partial N^{(k)}}{\partial x_2} \tag{10a}$$

$$u_y^{(k)} = -\frac{1}{2G^{(k)}}\left(\nu^{(k)}\Delta - \frac{\partial^2}{\partial x_3^2}\right)\frac{\partial L^{(k)}}{\partial x_2} - \frac{\partial N^{(k)}}{\partial x_1} \tag{10b}$$

$$u_z^{(k)} = -\frac{1}{G^{(k)}}\left(\Delta - \frac{\partial^2}{\partial x_3^2}\right)\frac{\partial L^{(k)}}{\partial x_3} + \frac{\partial}{\partial x_3}\left[\frac{1}{2G^{(k)}}\left(\nu^{(k)}\Delta - \frac{\partial^2}{\partial x_3^2}\right)L^{(k)}\right] \tag{10c}$$

Taking derivatives of Eq. (10a) and substituting into constitutive equations for isotropic material allows equations for stresses in terms of functions $L^{(k)}$ and $N^{(k)}$ to be written as

$$\sigma_{11}^{(k)} = \left(\nu^{(k)}\frac{\partial^2}{\partial x_2^2}\Delta + \frac{\partial^4}{\partial x_1^2\partial x_3^2}\right)L^{(k)} + 2G\frac{\partial^2 N^{(k)}}{\partial x_1\partial x_2} \tag{11a}$$

$$\sigma_{22}^{(k)} = \left(\nu^{(k)}\frac{\partial^2}{\partial x_1^2}\Delta + \frac{\partial^4}{\partial x_2^2\partial x_3^2}\right)L^{(k)} - 2G\frac{\partial^2 N^{(k)}}{\partial x_1\partial x_2} \tag{11b}$$

$$\sigma_{33}^{(k)} = \left(\Delta - \frac{\partial^2}{\partial x_3^2}\right)^2 L^{(k)} \tag{11c}$$

$$\sigma_{13}^{(k)} = -\left(\Delta - \frac{\partial^2}{\partial x_3^2}\right)\frac{\partial^2 L^{(k)}}{\partial x_1\partial x_3} + G^{(k)}\frac{\partial^2 N^{(k)}}{\partial x_2\partial x_3} \tag{11d}$$

$$\sigma_{23}^{(k)} = -\left(\Delta - \frac{\partial^2}{\partial x_3^2}\right)\frac{\partial^2 L^{(k)}}{\partial x_2\partial x_3} - G^{(k)}\frac{\partial^2 N^{(k)}}{\partial x_1\partial x_3} \tag{11e}$$

$$\sigma_{12}^{(k)} = -\left(\nu^{(k)}\Delta - \frac{\partial^2}{\partial x_3^2}\right)\frac{\partial^2 L^{(k)}}{\partial x_1\partial x_2} - G^{(k)}\left(\frac{\partial^2}{\partial x_1^2} - \frac{\partial^2}{\partial x_2^2}\right)N^{(k)} \tag{11f}$$

Functions $L^{(k)} = L^{(k)}(x_1,x_2,x_3)$ and $N^{(k)} = N^{(k)}(x_1,x_2,x_3)$ satisfy the following partial differential equations

$$\Delta\left(\frac{1}{G^{(k)}}\Delta L^{(k)}\right) - \frac{1}{1-\nu^{(k)}}\left(\Delta - \frac{\partial^2}{\partial x_3^2}\right)L^{(k)}\frac{d^2}{dx_3^2}\left(\frac{1}{G^{(k)}}\right) = 0 \tag{12a}$$

$$\Delta N^{(k)} + \frac{d}{dx_3}\ln G^{(k)}(x_3)\frac{\partial N^{(k)}}{\partial x_3} = 0 \tag{12b}$$

The solution of differential equations, Eq. (12a,b), can be aided through separating variables in the form of

$$L^{(k)}(x_1,x_2,x_3) = \psi_1^{(k)}(x_1,x_2)\phi_1^{(k)}(x_3), \tag{13a}$$

$$N^{(k)}(x_1,x_2,x_3) = \psi_2^{(k)}(x_1,x_2)\phi_2^{(k)}(x_3) \tag{13b}$$

This leads to transformation of Eq. (12a,b) into the Helmholtz's equation for functions $\psi_1^{(k)}(x_1,x_2)$ and $\psi_2^{(k)}(x_1,x_2)$, and the forth- and the second-order ordinary differential equations for functions $\phi_1^{(k)}(x_3)$ and $\phi_2^{(k)}(x_3)$.

For sinusoidal loading, Eq. (7), and Navier-type boundary conditions on the edges, Eq. (9), functions $\psi_1^{(k)}(x_1,x_2)$ and $\psi_2^{(k)}(x_1,x_2)$ can be chosen as

$$\psi_1^{(k)}(x_1,x_2)=\sin\frac{\pi m x_1}{a}\sin\frac{\pi n x_2}{b},\quad k=1,\dots,p \tag{14a}$$

$$\psi_2^{(k)}(x_1,x_2)=\cos\frac{\pi m x_1}{a}\cos\frac{\pi n x_2}{b},\quad k=1,\dots,p \tag{14b}$$

Then boundary conditions on the edges, Eq. (9a,b) are satisfied exactly for any numbers $n,\ m$.

For the shear moduli $G^{(k)}=G^{(k)}(x_3)$ that are exponential functions of the thickness co-ordinate in the form of Eq. (3), equations Eq. (11a,b) are reduced to the following ordinary differential equations with constant coefficients with respect to functions $\phi_1^{(k)}(x_3)$ and $\phi_2^{(k)}(x_3)$

$$h^4\frac{d^4\phi_1^{(k)}}{dx_3^4}-2\gamma^{(k)}h^3\frac{d^3\phi_1^{(k)}}{dx_3^3}+[\gamma^{(k)^2}-2\alpha^2h^2]h^2\frac{d^2\phi_1^{(k)}}{dx_3^2}+2\alpha^2\gamma^{(k)}h^3\frac{d\phi_1^{(k)}}{dx_3}+\alpha^2h^2\left(\alpha^2h^2+\frac{\nu^{(k)}}{1-\nu^{(k)}}\gamma^{(k)^2}\right)\phi_1^{(k)}=0 \tag{15a}$$

$$h^2\frac{d^2\phi_2^{(k)}}{dx_3^2}+\gamma^{(k)}h\frac{d\phi_2^{(k)}}{dx_3}-\alpha^2h^2\phi_2^{(k)}=0,\quad \alpha=\pi\sqrt{\left(\frac{m}{a}\right)^2+\left(\frac{n}{b}\right)^2} \tag{15b}$$

Solving the above fourth- and second-order ordinary differential equations following standard procedures, functions $\phi_1^{(k)}(x_3)$ and $\phi_2^{(k)}(x_3)$ are found as

$$\phi_1^{(k)}(x_3)=h^4\exp\left(\frac{\gamma^{(k)}x_3}{2h}\right)\left[A_1^{(k)}\cosh\frac{\lambda^{(k)}x_3}{h}\cos\frac{\mu^{(k)}x_3}{h}+A_2^{(k)}\sinh\frac{\lambda^{(k)}x_3}{h}\cos\frac{\mu^{(k)}x_3}{h}++A_3^{(k)}\cosh\frac{\lambda^{(k)}x_3}{h}\sin\frac{\mu^{(k)}x_3}{h}+A_4^{(k)}\sinh\frac{\lambda^{(k)}x_3}{h}\sin\frac{\mu^{(k)}x_3}{h}\right] \tag{16a}$$

$$\phi_2^{(k)}(x_3)=h^2\exp\left(-\frac{\gamma^{(k)}x_3}{2h}\right)\left[A_5^{(k)}\cosh\frac{\beta^{(k)}x_3}{h}+A_6^{(k)}\sinh\frac{\beta^{(k)}x_3}{h}\right] \tag{16b}$$

Here $A_j^{(k)}(j=1,\dots,6;\ k=1,\dots,p)$ are arbitrary constants that can be determined from the stress and displacement continuity conditions at the interfaces, Eq. (6), and the boundary conditions on the top and bottom surfaces of the panel, Eqs. (7) and (8). Coefficients $\lambda^{(k)}$ and $\mu^{(k)}$, and $\beta^{(k)}$, are the roots of characteristic equations corresponding to Eqs. (15a) and (15b), respectively. Expressions for them are given in Appendix A.

Substitution of functions $\psi_1^{(k)}(x,y)$ and $\psi_2^{(k)}(x,y)$, Eq. (10), and functions $\phi_1^{(k)}(z)$ and $\phi_2^{(k)}(z)$, Eq. (13a,b), into Eq. (9), and then into Eq. (6), gives the following expressions for displacements in a sandwich panel with functionally graded core.

$$u_1^{(k)}=\sum_{m=1}^{\infty}\sum_{n=1}^{\infty}\sum_{j=1}^{6}A_{j,mn}^{(k)}U_{1,jmn}^{(k)}(x_3)\cos\frac{\pi m x_1}{a}\sin\frac{\pi n x_2}{b} \tag{17a}$$

$$u_2^{(k)}=\sum_{m=1}^{\infty}\sum_{n=1}^{\infty}\sum_{j=1}^{6}A_{j,mn}^{(k)}U_{2,jmn}^{(k)}(x_3)\sin\frac{\pi m x_1}{a}\cos\frac{\pi n x_2}{b} \tag{17b}$$

$$u_3^{(k)}=\sum_{m=1}^{\infty}\sum_{n=1}^{\infty}\sum_{j=1}^{6}A_{j,mn}^{(k)}U_{3,jmn}^{(k)}(x_3)\sin\frac{\pi m x_1}{a}\sin\frac{\pi n x_2}{b} \tag{17c}$$

For stresses in any layer of the panel the expressions are

$$\sigma_{33}^{(k)}=\sum_{m=1}^{\infty}\sum_{n=1}^{\infty}\sum_{j=1}^{6}A_{j,mn}^{(k)}P_{33,jmn}^{(k)}(x_3)\sin\frac{\pi m x_1}{a}\sin\frac{\pi n x_2}{b} \tag{18a}$$

$$\sigma_{13}^{(k)}=\sum_{m=1}^{\infty}\sum_{n=1}^{\infty}\sum_{j=1}^{6}A_{j,mn}^{(k)}P_{13,jmn}^{(k)}(x_3)\cos\frac{\pi m x_1}{a}\sin\frac{\pi n x_2}{b} \tag{18b}$$

$$\sigma_{23}^{(k)}=\sum_{m=1}^{\infty}\sum_{n=1}^{\infty}\sum_{j=1}^{6}A_{j,mn}^{(k)}P_{23,jmn}^{(k)}(x_3)\sin\frac{\pi m x_1}{a}\cos\frac{\pi n x_2}{b} \tag{18c}$$

$$\sigma_{11}^{(k)}=\sum_{m=1}^{\infty}\sum_{n=1}^{\infty}\sum_{j=1}^{6}A_{j,mn}^{(k)}P_{11,jmn}^{(k)}(x_3)\sin\frac{\pi m x_1}{a}\sin\frac{\pi n x_2}{b} \tag{18d}$$

$$\sigma_{22}^{(k)}=\sum_{m=1}^{\infty}\sum_{n=1}^{\infty}\sum_{j=1}^{6}A_{j,mn}^{(k)}P_{22,jmn}^{(k)}(x_3)\sin\frac{\pi m x_1}{a}\sin\frac{\pi n x_2}{b} \tag{18e}$$

$$\sigma_{12}^{(k)}=\sum_{m=1}^{\infty}\sum_{n=1}^{\infty}\sum_{j=1}^{6}A_{j,mn}^{(k)}P_{12,jmn}^{(k)}(x_3)\cos\frac{\pi m x_1}{a}\cos\frac{\pi n x_2}{b} \tag{18f}$$

Here $A_{j,mn}^{(k)}$ are arbitrary constants and $U_{1,jmn}^{(k)}$, $U_{2,jmn}^{(k)}$, $U_{3,jmn}^{(k)}$, $P_{33,jmn}^{(k)}$, $P_{13,jmn}^{(k)}$, $P_{23,jmn}^{(k)}$, $P_{11,jmn}^{(k)}$, $P_{22,jmn}^{(k)}$ and $P_{12,jmn}^{(k)}$ are functions given in Appendix.

Substitution of Eqs. (17)–(18) into the stress and displacement continuity conditions, Eq. (6), at the interfaces $x_3=x_3^{(k)}(k=1,\dots p-1)$, and boundary conditions, Eq. (8), at the top ($x_3=h$) and bottom ($x_3=0$) surfaces of the panel produces a set of $6\times p$ linear algebraic equations with respect to arbitrary constants $A_{j,mn}^{(k)}$ for any combination of m and n. These are solved in Matlab using LU decomposition method. Boundary conditions at the edges of the panel, Eq. (9a,b), are satisfied exactly.

4. Results and discussion

4.1. Convergence and validation

As already mentioned in Section 2, through the coefficients of the exponential functions, the number and thickness of the layers in the piecewise-exponential model, many different variations of shear modulus through the thickness can be modelled. The number of layers required for a given accuracy can be established through convergence study. In this paper, the convergence study is performed on a thick square panel with $a/h_0=b/h_0=3$ and through-thickness variation of shear modulus shown in Fig. 2. The panel is split into p layers, layers 1 and p being the face sheets, and layers 2 to (p - 1) being core layers of equal thickness. The thickness of the face sheets is $h_f=0.05h_0$ and the Poisson's ratios are taken as $\nu^{(k)}=0.3,\ k=1,\dots,p$. The following stresses and displacements in the panel are calculated for a range of p values: normal stresses $\sigma_{33}(0.5a,0.5b,-0.3h)$ and $\sigma_{11}(0.5a,0.5b,0.5h)$; transverse shear stress $\sigma_{13}(0.,0.5b,0.75h)$; in-plane displacement $u_1(0.,0.5b,-0.8h)$; transverse displacement $u_3(0.5a,0.5b,0.2h)$.

Table 1 shows stresses and displacements in the panel with linear variation of the core stiffness through the thickness, which corresponds to the power law index $r=1$. For this case, the solution begins to break down if over 90 layer are used, the reason being that if linear variation is modelled by too many exponential layers, the solution begins to approach a 'stepwise' one. The results

Table 1
Stresses and displacements in the panel with power law index $r = 1$.

Number of layers	$r = 1$				
	σ_{33}	σ_{11}	σ_{13}	u_1	u_3
2	−0.328722	−0.29850	−0.43650	−1.04719	−6.93501
4	−0.3226956	−0.35856	−0.42185	−0.95695	−5.84836
6	−0.3202807	−0.40507	−0.41548	−0.94183	−5.53262
8	−0.3191229	−0.42722	−0.41236	−0.93567	−5.39095
10	−0.3184911	−0.43766	−0.41064	−0.93254	−5.31408
20	−0.3174996	−0.45484	−0.40782	−0.92789	−5.19567
30	−0.3172869	−0.45856	−0.40718	−0.92694	−5.17021
40	−0.3172088	−0.45994	−0.40694	−0.92660	−5.16087
50	−0.3171721	−0.46056	−0.40683	−0.92643	−5.15646
60	−0.3171524	−0.46089	−0.40677	−0.92635	−5.15403
70	−0.3171403	−0.46110	−0.40673	−0.92630	−5.15256
80	−0.3171310	−0.46124	−0.40670	−0.92625	−5.15162
90	−0.3171268	−0.46135	−0.40669	−0.92624	−5.15094
100	−0.3191334	−0.43877	−0.33737	−0.81025	−2.19198
200	−0.3173617	−0.44951	−0.33769	−0.80638	−2.15027
400	−0.3280116	−0.76586	0.02463	−0.33680	−0.49464

Table 2
Stresses and displacements in the panel with power law index $r = 2$.

Number of layers	$r = 2$				
	σ_{33}	σ_{11}	σ_{13}	u_1	u_3
2	−0.3287	−0.2985	−0.4365	−1.0472	−6.9350
4	−0.3284	−0.3009	−0.4358	−1.0431	−6.8746
6	−0.3294	−0.2738	−0.4378	−1.0352	−6.9972
8	−0.3299	−0.2613	−0.4397	−1.0328	−7.0779
10	−0.3302	−0.2541	−0.4408	−1.0317	−7.1246
20	−0.3306	−0.2447	−0.4424	−1.0303	−7.1913
30	−0.3307	−0.2428	−0.4427	−1.0300	−7.2041
40	−0.3308	−0.2421	−0.4428	−1.0299	−7.2086
50	−0.3308	−0.2418	−0.4429	−1.0299	−7.2107
100	−0.3308	−0.2414	−0.4430	−1.0298	−7.2135
200	−0.3308	−0.2413	−0.4430	−1.0298	−7.2142
400	−0.3308	−0.2413	−0.4430	−1.0298	−7.2144

Table 3
Stresses and displacements in the panel with power law index $r = 3$.

Number of layers	$r = 3$				
	σ_{33}	σ_{11}	σ_{13}	u_1	u_3
2	−0.3287	−0.2985	−0.4365	−1.0472	−6.9350
4	−0.3326	−0.2689	−0.4458	−1.1005	−7.9101
6	−0.3345	−0.2245	−0.4511	−1.0965	−8.2842
8	−0.3351	−0.2166	−0.4528	−1.0936	−8.4019
10	−0.3353	−0.2103	−0.4536	−1.0920	−8.4551
20	−0.3356	−0.2035	−0.4548	−1.0896	−8.5225
30	−0.3357	−0.2023	−0.4550	−1.0892	−8.5350
40	−0.3357	−0.2018	−0.4551	−1.0890	−8.5393
50	−0.3357	−0.2016	−0.4551	−1.0889	−8.5414
100	−0.3357	−0.2013	−0.4551	−1.0888	−8.5441
200	−0.3357	−0.2012	−0.4552	−1.0888	−8.5448
400	−0.3357	−0.2012	−0.4552	−1.0888	−8.5450

for the power law variation of the core stiffness through the thickness, with index $r = 2,\ 3,\ 4$, are shown in Tables 2–4, respectively. In all cases, the difference between stress and displacement values calculated for $p = 20$ and $p = 30$ is less than 1%, and the number of layers in the piecewise-exponential model is therefore fixed at $p = 20$ henceforth.

Validation of the proposed 3-D piecewise-exponential model is given through comparison with elasticity solutions available in literature. Reddy (2000) and Zenkour (2006) give numerical results for the transverse deflections and stresses in an isotropic functionally graded plate with power law variation in modulus subject to sinusoidal loading of the form

Table 4
Stresses and displacements in the panel with power law index $r = 4$.

Number of layers	Power law index $r = 4$				
	σ_{33}	σ_{11}	σ_{13}	u_1	u_3
2	−0.3287	−0.2985	−0.4365	−1.0472	−6.9350
4	−0.3354	−0.2522	−0.4523	−1.1322	−8.8138
6	−0.3369	−0.2224	−0.4566	−1.1381	−9.1764
8	−0.3372	−0.2221	−0.4573	−1.1360	−9.2918
10	−0.3374	−0.2191	−0.4578	−1.1345	−9.3474
20	−0.3376	−0.2158	−0.4586	−1.1319	−9.4201
30	−0.3377	−0.2154	−0.4587	−1.1314	−9.4337
40	−0.3377	−0.2154	−0.4588	−1.1312	−9.4385
50	−0.3377	−0.2153	−0.4588	−1.1311	−9.4407
100	−0.3377	−0.2151	−0.4589	−1.1310	−9.4436
200	−0.3377	−0.2151	−0.4589	−1.1310	−9.4444
400	−0.3377	−0.2151	−0.4589	−1.1309	−9.4446

Table 5
Comparison with generalised shear deformation theory (GSDT) of Zenkour (2006) for a range of power law indexes r.

r	Approach	$\bar{u}_3$	$\bar{\sigma}_{11}$	$\bar{\sigma}_{13}$	$\bar{\sigma}_{12}$
Ceramic	GSDT	0.296	1.9955	0.2462	0.7065
	Present	0.2917	2.0044	0.2383	0.7014
	% Difference	1.4527	−0.4460	3.2088	0.7219
1	GSDT	0.5889	3.087	0.2462	0.611
	Present	0.587	3.1052	0.2383	0.6104
	% Difference	0.3226	−0.5896	3.2088	0.0982
2	GSDT	0.7573	3.6094	0.2265	0.5441
	Present	0.7527	3.6208	0.2256	0.544
	% Difference	0.6074	−0.3158	0.3974	0.0184
3	GSDT	0.8377	3.8742	0.2107	0.5525
	Present	0.8343	3.8901	0.2197	0.5501
	% Difference	0.4059	−0.4104	−4.2715	0.4344
4	GSDT	0.8819	4.0693	0.2029	0.5667
	Present	0.8787	4.0825	0.2176	0.5632
	% Difference	0.3629	−0.3244	−7.2449	0.6176
5	GSDT	0.9118	4.2488	0.2017	0.5755
	Present	0.908	4.2538	0.2169	0.5721
	% Difference	0.4168	−0.1177	−7.5359	0.5908
6	GSDT	0.9356	4.4244	0.2041	0.5803
	Present	0.9307	4.4176	0.2167	0.5775
	% Difference	0.5237	0.1537	−6.1734	0.4825
7	GSDT	0.9562	4.5971	0.2081	0.5834
	Present	0.95	4.576	0.2166	0.581
	% Difference	0.6484	0.4590	−4.0846	0.4114
8	GSDT	0.975	4.7661	0.2124	0.5856
	Present	0.9673	4.7287	0.2166	0.5835
	% Difference	0.7897	0.7847	−1.9774	0.3586
9	GSDT	0.9925	4.9303	0.2164	0.5875
	Present	0.9832	4.8748	0.2166	0.5856
	% Difference	0.9370	1.1257	−0.0924	0.3234
Metal	GSDT	1.607	1.9955	0.2462	0.7065
	Present	1.5833	2.0044	0.2383	0.7014
	% Difference	1.4748	−0.4460	3.2088	0.7219

$$q(x_1, x_2) = q_0 \sin\left(\frac{\pi x_1}{a}\right) \sin\left(\frac{\pi x_2}{b}\right) \tag{19}$$

In this case it is assumed that the x_3-axis is positive upwards from the mid-plane of the plate and that the plate varies from pure metal on the bottom surface to pure ceramic on the top surface, with Young's modulus a function of the volume fraction of the constituent materials.

$$E(x_3) = E_m + (E_c - E_m)\left(\frac{2x_3 + h}{2h}\right)^r \tag{20}$$

where E_m and E_c are the Young's moduli of the metal and ceramic respectively and r is the power law index (if set equal to zero then plate will be pure ceramic).

Table 6
Comparison with higher order shear deformation theory (HSDT) of Reddy (2000) for a range of power law indices r.

r	Approach	$\bar{u}_3$	$\bar{\sigma}_{11}$	$\bar{\sigma}_{13}$	$\bar{\sigma}_{12}$
Ceramic	HSDT	0.294	1.98915	0.23778	0.70557
	Present	0.2917	2.0044	0.2383	0.7014
	% Difference	0.7823	−0.7667	−0.2187	0.5910
1	HSDT	0.58895	3.08501	0.23817	0.61111
	Present	0.587	3.1052	0.2383	0.6104
	% Difference	0.3311	−0.6545	−0.0546	0.1162
2	HSDT	0.75747	3.60664	0.22568	0.54434
	Present	0.7527	3.6208	0.2256	0.544
	% Difference	0.6297	−0.3926	0.0354	0.0625
5	HSDT	0.90951	4.24293	0.21609	0.57368
	Present	0.908	4.2538	0.2169	0.5721
	% Difference	0.1660	−0.2562	−0.3748	0.2754
Metal	HSDT	1.59724	1.98915	0.23778	0.70557
	Present	1.5833	2.0044	0.2383	0.7014
	% Difference	0.8728	−0.7667	−0.2187	0.5910

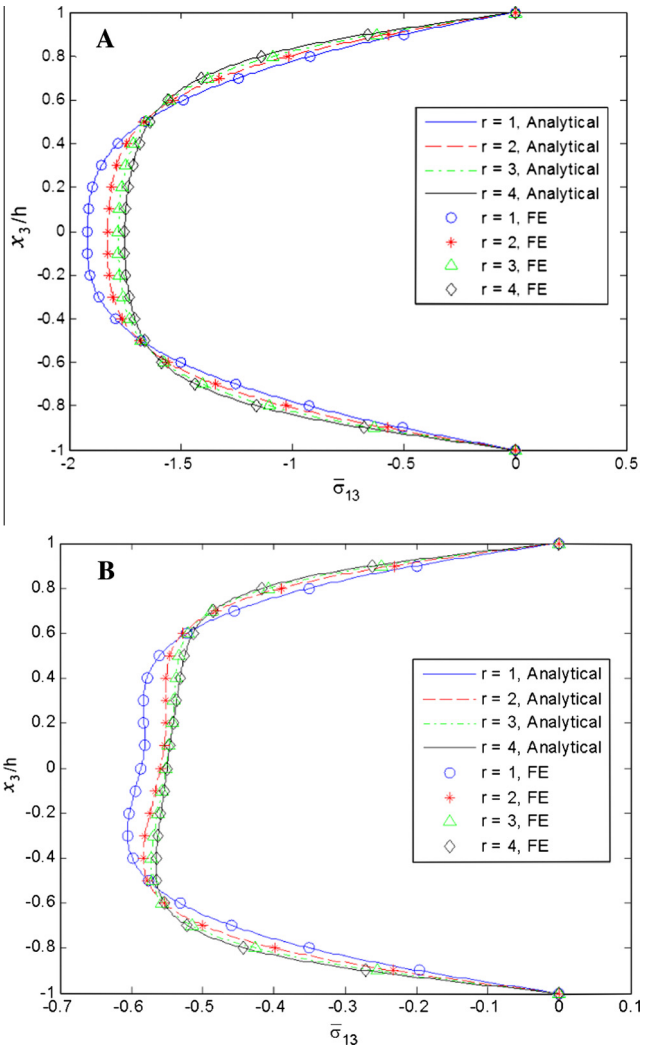

Fig. 3. Through-thickness variation of the normalised transverse shear stress $\bar{\sigma}_{13}\ (0, 0.5b, x_3)$ for a range of power law indexes ($r = 1,\ 2,\ 3,\ 4$) in: (A) thin panel; (B) thick panel.

Tables 5 and 6 contain normalised transverse deflections and stresses of a functionally graded square thin plate with aspect ratio $\frac{a}{h} = 10$, comprising aluminium (metal) and alumina (ceramics)

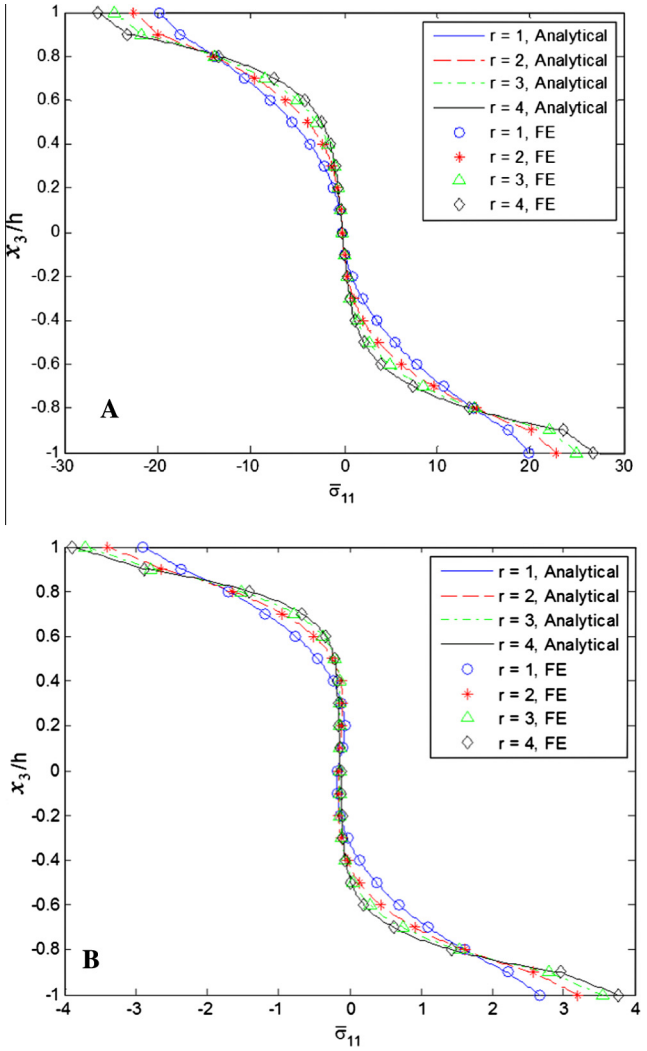

Fig. 4. Through-thickness variation of the normalised in-plane normal stress $\bar{\sigma}_{11}\ (0.5a, 0.5b, x_3)$ for a range of power law indexes ($r = 1,\ 2,\ 3,\ 4$) in: (A) thin panel; (B) thick panel.

with the following elastic properties: $E_m = 70$ GPa, $E_c = 380$ GPa and constant Poisson's ratio $\nu = 0.3$. Results are given for generalised shear deformation theory (Zenkour, 2006), higher order shear deformation theory (Reddy, 2000) and the current 3-D piecewise exponential model. In all cases normalisation is carried out in an identical fashion to Reddy (2000):

$$\bar{u}_3 = u_3(a/2, b/2, h)(10h^3E_c/a^4q_0);$$
$$\bar{\sigma}_{11} = \sigma_{11}(a/2, b/2, h/2)(h/aq_0);$$

$$\bar{\sigma}_{12} = \sigma_{12}(0, 0, -h/3)(h/aq_0); \quad \bar{\sigma}_{13} = \sigma_{13}(0, b/2, 0)(h/aq_0).$$

It can be seen that results obtained used the proposed 3-D piecewise exponential model are in good agreement with Zenkour (2006), whilst in excellent agreement with Reddy (2000), which is seen by many researchers as a benchmark method (Birman and Byrd, 2007). It is worth pointing out the proposed piecewise exponential model is based on 3-D elasticity theory and therefore is applicable to much thicker plates that those considered within shear deformation theories.

To further verify the 3-D piecewise exponential model, a finite element (FE) analysis of the same problem has been carried out using Abaqus software. In order to accurately model the problem,

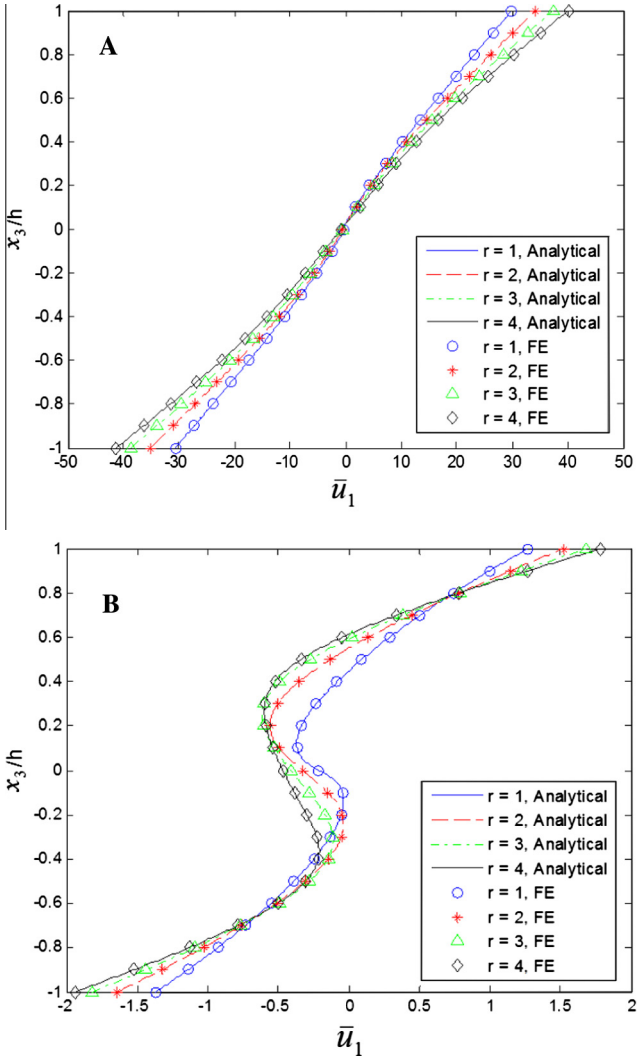

Fig. 5. Through-thickness variation of the normalised in-plane displacement $\bar{u}_1\ (0, 0.5b, x_3)$ for a range of power law indexes ($r = 1,\ 2,\ 3,\ 4$) in: (A) thin panel; (B) thick panel.

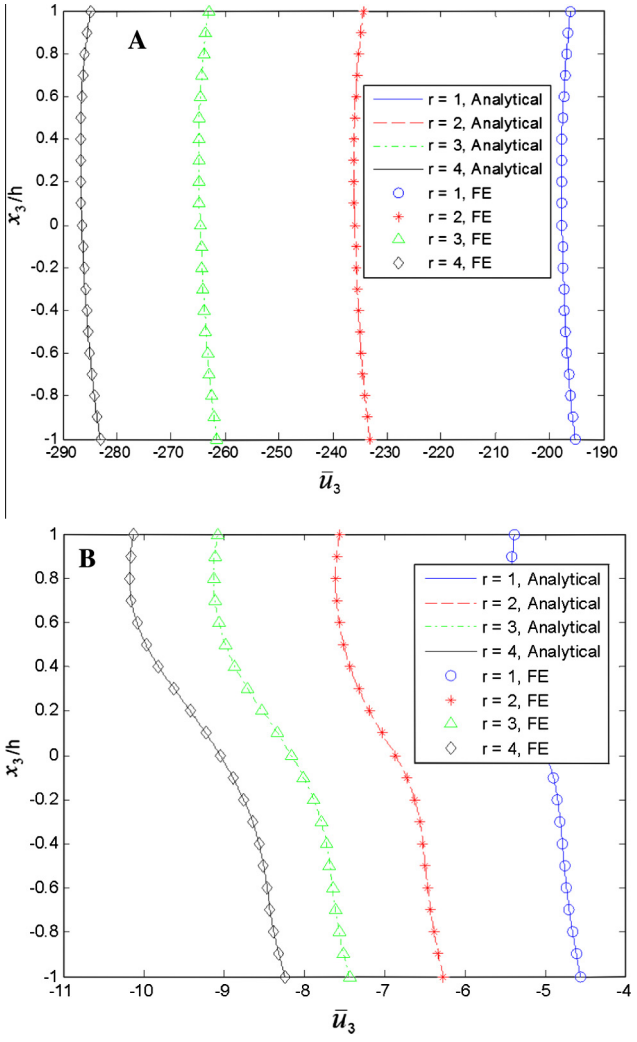

Fig. 6. Through-thickness variation of the normalised transverse displacement $\bar{u}_3\ (0.5a, 0.5b, x_3)$ for a range of power law indexes ($r = 1,\ 2,\ 3,\ 4$) in: (A) thin panel; (B) thick panel.

a mesh utilising 20 node quadrilateral elements is used. The face sheets comprise $20 \times 20 \times 2$ homogeneous elements, whilst each half of the core is modelled by $20 \times 20 \times 10$ elements whose stiffness is graded in the x_3 direction. In Abaqus, elements with graded stiffness are introduced through a user defined material (UMAT) subroutine. This subroutine is written in FORTRAN and is called at all material calculation points, and to define the mechanical constitutive behaviour of the material including the power law variation in modulus in this case. Numerical results of FE analysis are shown in Figs. 3–6, where the analytical solutions are represented by connected lines, whist the FE solutions are shown as marker points. Excellent agreement is observed between analytical and FE results.

4.2. Comparative study of thick and thin panels

In this subsection, a comparative study based on the new piecewise exponential model is presented. It was carried out with the view to establish the effect of sandwich panel thickness and stiffness gradient of the core on the stresses and displacements in the panel. To this end, two sandwich panels with graded core were examined: a thin panel ($a/h_0 = b/h_0 = 9$) and a thick panel ($a/h_0 = b/h_0 = 3$); for both panels, the power law variation in the core stiffness was considered, corresponding to the power law index $r = 1,\ 2,\ 3,\ 4$. The thickness of the face sheets is $h_f = 0.05h_0$ and the Poisson's ratios are taken as $\nu^{(k)} = 0.3$, $k = 1, \ldots, 20$.

The effect of varying power index r on stresses and displacements in the panel with graded core can be seen in Figs. 3–6 which show through thickness variation of the normalised stresses $\bar{\sigma}_{ij} = \sigma_{ij}/q_0$ and normalised displacements $\bar{u}_i = \frac{G_{face} u_i}{q_0 h}$, for four different values of $r = 1,\ 2,\ 3,\ 4$. Through-thickness variation of the normalised transverse shear stress $\bar{\sigma}_{13}$ (Fig. 3) shows that increasing the value of power law index r (and therefore decreasing the stiffness near the centre of the panel) has the effect of reducing the transverse shear stress in the core. Through-thickness variation of the normalised in-plane normal stress $\bar{\sigma}_{11}$ (Fig. 4) is clearly affected by varying power law index r. Both in thin and thick panels it can be seen that by increasing power law index r, the stresses in the face sheets increase, whilst decreasing in the core. A similar observation can be made for normalised in-plane shear stress $\bar{\sigma}_{12}$.

Figs. 5 and 6 show through-thickness variation of the normalised in-plane displacement $\bar{u}_1$ and normalised transverse displacement $\bar{u}_3$. It can be seen that as the power law index r is increased (and therefore the stiffness near the centre of the panel is decreased), that both of these displacement components increase throughout the panel. It should be noted that in-plane displacements are highly non-linear, particularly in thicker panels.

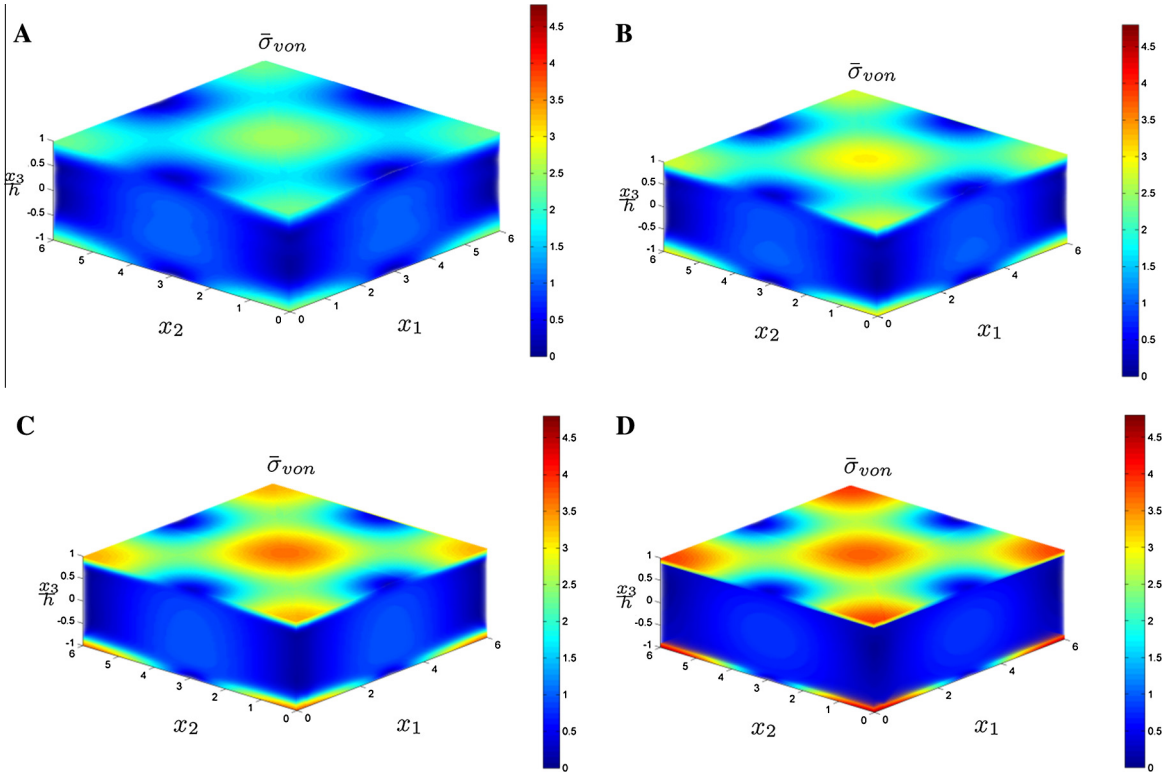

Fig. 7. Effect of power law index on distribution of von Mises stress $\bar{\sigma}_{von}$ throughout panel: (A) power law index $r = 1$; (B) power law index $r = 2$; (C) power law index $r = 5$; (D) power law index $r = 25$. Thick panel $(a/h_0 = b/h_0 = 3)$ $r = 25$.

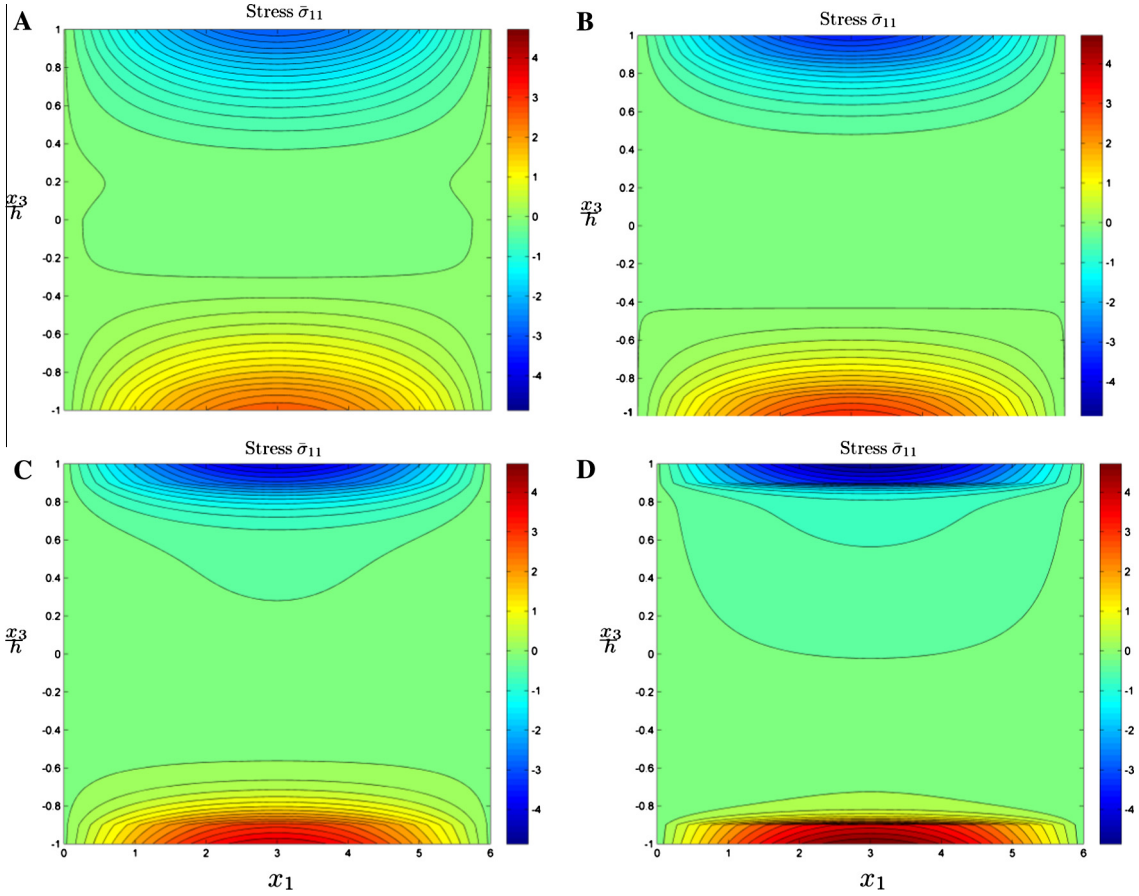

Fig. 8. Effect of power law index on through thickness variation of normalised in-plane normal stress $\bar{\sigma}_{11}$ on a central vertical section $x_2 = b/2$: (A) power law index $r = 1$; (B) power law index $r = 2$; (C) power law index $r = 5$; (D) power law index $r = 25$. Thick panel $(a/h_0 = b/h_0 = 3)$.

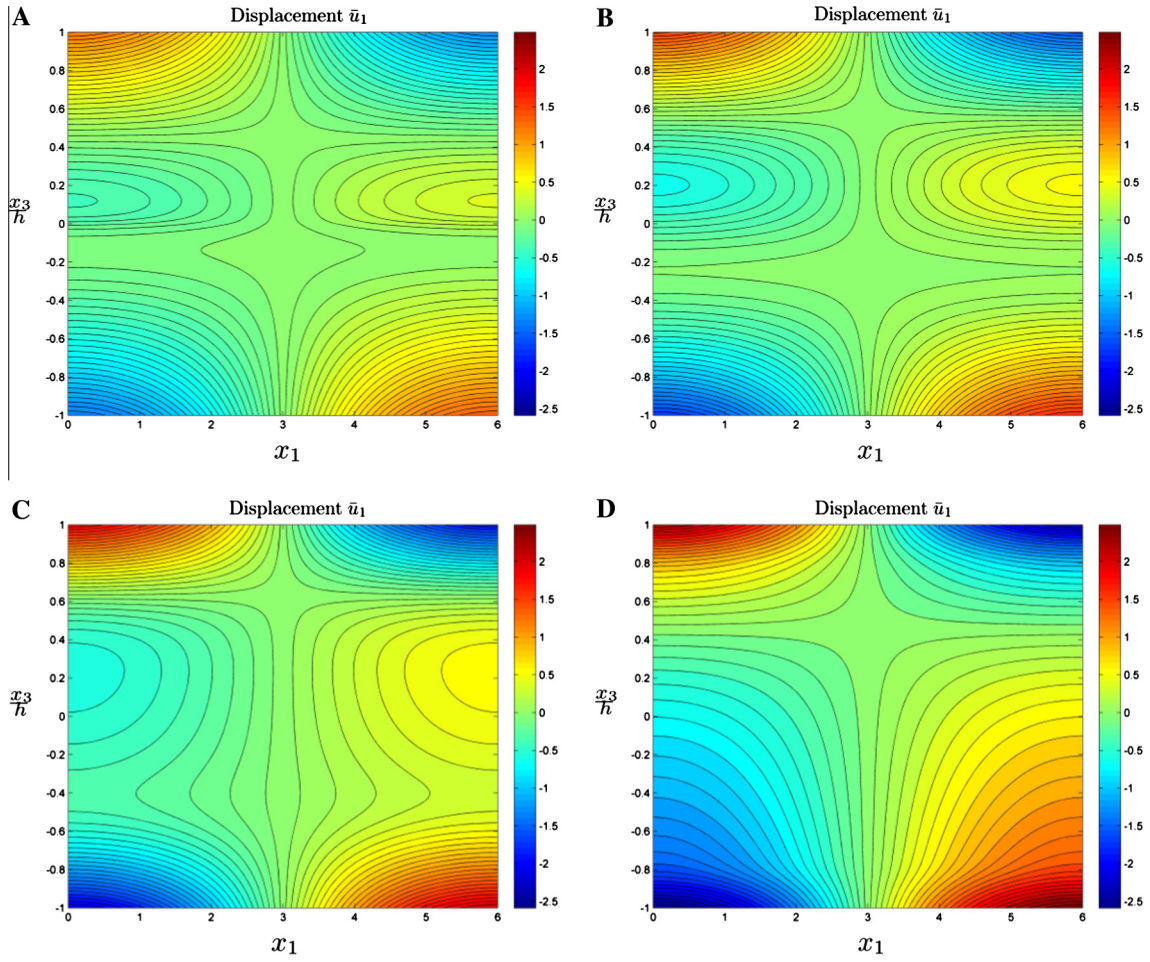

Fig. 9. Effect of power law index on through thickness variation of normalised in-plane displacement $\bar{u}_1$ on a central vertical section $x_2 = b/2$: (A) power law index $r = 1$; (B) power law index $r = 2$; (C) power law index $r = 5$; (D) power law index $r = 25$. Thick panel $(a/h_0 = b/h_0 = 3)$.

The effect of varying power law index of the core in thick panels $(a/h_0 = b/h_0 = 3)$ is further explored in Fig. 7–9. Fig. 7 shows the distribution of von Mises stress on the panel, with increasing power law index, r, whilst Fig. 8 highlights the in-plane normal stress $\bar{\sigma}_{11}$ on a central vertical section of the panel. In both figures it is clear that as the power law index is increased, both in-plane normal and in-plane shear stresses increase. This increase in stress is because as the power law index is increased, the stiffness at any location through the thickness of the core is decreased. This leads to a reduction in flexural rigidity of the panel and increased bending stresses particularly within the face sheets. It should also be noted that as the power law becomes sufficiently large, the solution tends towards the solution for a panel containing homogenous core with a discontinuity present in in-plane normal and in-plane shear stresses. Therefore in reality graded materials with a high power law variation in stiffness should be avoided.

Fig. 9 shows through thickness variation of the normalised in-plane displacement $\bar{u}_1$. It can be seen that by increasing power law index r (and therefore decreasing the stiffness near the centre of the panel) causes an increase in displacement. It should be noted that in all of the considered cases, the in-plane displacements are highly non-linear and non-symmetric with respect to the mid-plane.

5. Conclusions

The paper presents a piecewise exponential model for functionally graded plates and sandwich panels with graded core which can be used to simulate any through thickness variation in stiffness provided it can be represented by a smooth function. The new model is developed in the framework of three-dimensional elasticity theory and can therefore be applied to analysis of thick plates and sandwich panels. The model is fully validated through comparison with results from the literature for thin plates and a finite element study for both thick and thin plates. Based on the new piecewise exponential model, three-dimensional elasticity analysis of sandwich panel with power law variation in the core stiffness properties is performed. A comparative study is carried out to examine the effect of panel thickness and varying the power law index on the stresses and displacements in the panel. Numerical results clearly demonstrate that the proposed piecewise exponential model, being based on a three-dimensional elasticity solution, can accurately capture the specifics of stress and displacement fields in thick sandwich panels. Thus the proposed piecewise exponential model has an advantage over the plate theory-based approaches which cannot be used for thick plates.

Acknowledgements

Financial support of this research by the EPSRC (Engineering and Physical Sciences Research Council) (EP/P503299/1, EP/P503930/1), United Kingdom, is gratefully acknowledged.

Appendix A

Coefficients $\lambda^{(k)}$ and $\mu^{(k)}$, and $\beta^{(k)}$ involved in Eq. (15)

$$\begin{pmatrix}\lambda^{(k)}\\ \mu^{(k)}\end{pmatrix}=\sqrt{\frac{1}{2}\left(\pm\beta^{(k)^2}+\sqrt{\beta^{(k)^4}+\gamma^{(k)^2}\alpha^2h^2\frac{\nu^{(k)}}{1-\nu^{(k)}}}\right)},$$

$$\beta^{(k)}=\sqrt{\frac{\gamma^{(k)^2}}{4}+\alpha^2h^2},$$

$$\alpha=\pi\sqrt{\left(\frac{m}{a}\right)^2+\left(\frac{n}{b}\right)^2},$$

$$g^{(k)}=\Gamma^{(k)}(h)$$

Functions $U^{(k)}_{i,jmn}$ and $P^{(k)}_{rt,jmn}$ involved in Eqs. (17a–c) and (18a–f)

$$U^{(k)}_{1,jmn}(\bar{x}_3)=-\frac{q_{mn}h}{2g^{(k)}}\frac{\pi mh}{a}\exp[-\gamma^{(k)}(\bar{x}_3-1)]\times\left[-\nu^{(k)}\alpha^2h^2f^{(k)}_j(\bar{x}_3)+(\nu^{(k)}-1)\frac{d^2}{d\bar{x}_3^2}f^{(k)}_j(\bar{x}_3)\right]$$

$$U^{(k)}_{2,jmn}(\bar{x}_3)=-\frac{q_{mn}h}{2g^{(k)}}\frac{\pi nh}{b}\exp[-\gamma^{(k)}(\bar{x}_3-1)]\times\left[-\nu^{(k)}\alpha^2h^2f^{(k)}_j(\bar{x}_3)+(\nu^{(k)}-1)\frac{d^2}{d\bar{x}_3^2}f^{(k)}_j(\bar{x}_3)\right]$$

$$U^{(k)}_{3,jmn}(\bar{x}_3)=-\frac{q_{mn}h}{2g^{(k)}}\frac{\pi mh}{a}\exp[-\gamma^{(k)}(\bar{x}_3-1)]\times\left[(\nu^{(k)}-1)\left(-\gamma^{(k)}\frac{d^2}{d\bar{x}_3^2}f^{(k)}_j(\bar{x}_3)+\frac{d^3}{d\bar{x}_3^2}f^{(k)}_j(\bar{x}_3)\right)-\alpha^2h^2\left((\nu^{(k)}-2)\frac{d}{d\bar{x}_3}f^{(k)}_j(\bar{x}_3)-\nu^{(k)}\gamma^{(k)}f^{(k)}_j(\bar{x}_3)\right)\right],\quad j=1,\dots,4;$$

$$U^{(k)}_{1,jmn}(\bar{x}_3)=-\frac{q_{mn}h}{g^{(k)}}\frac{\pi nh}{b}f^{(k)}_j(\bar{x}_3)$$

$$U^{(k)}_{2,jmn}(\bar{x}_3)=\frac{q_{mn}h}{g^{(k)}}\frac{\pi mh}{a}f^{(k)}_j(\bar{x}_3)$$

$$U^{(k)}_{3,jmn}(\bar{x}_3)=0,\quad j=5,\ 6;$$

$$P^{(k)}_{33,jmn}(\bar{x}_3)=q_{mn}\alpha^4h^4f^{(k)}_j(\bar{x}_3)$$

$$P^{(k)}_{13,jmn}(\bar{x}_3)=q_{mn}\alpha^2h^2\left(\frac{\pi mh}{a}\right)\frac{d}{d\bar{x}_3}f^{(k)}_j(\bar{x}_3)$$

$$P^{(k)}_{23,jmn}(\bar{x}_3)=q_{mn}\alpha^2h^2\left(\frac{\pi nh}{b}\right)\frac{d}{d\bar{x}_3}f^{(k)}_j(\bar{x}_3)$$

$$P^{(k)}_{11,jmn}(\bar{x}_3)=q_{mn}\left[\nu^{(k)}\alpha^2h^2\left(\frac{\pi nh}{b}\right)^2f^{(k)}_j(\bar{x}_3)-\nu^{(k)}\left(\frac{\pi nh}{b}\right)^2\frac{d^2}{d\bar{x}_3^2}f^{(k)}_j(\bar{x}_3)-\left(\frac{\pi mh}{a}\right)^2\frac{d^2}{d\bar{x}_3^2}f^{(k)}_j(\bar{x}_3)\right]$$

$$P^{(k)}_{22,j}(\bar{x}_3)=q_{mn}\left[\nu^{(k)}\alpha^2h^2\left(\frac{\pi mh}{a}\right)^2f^{(k)}_j(\bar{x}_3)-\nu^{(k)}\left(\frac{\pi mh}{a}\right)^2\frac{d^2}{d\bar{x}_3^2}f^{(k)}_j(\bar{x}_3)-\left(\frac{\pi nh}{b}\right)^2\frac{d^2}{d\bar{x}_3^2}f^{(k)}_j(\bar{x}_3)\right]$$

$$P^{(k)}_{12,jmn}(\bar{x}_3)=q_{mn}\left(\frac{\pi mh}{a}\right)\left(\frac{\pi nh}{b}\right)\left[\nu^{(k)}\alpha^2h^2f^{(k)}_j(\bar{x}_3)+(1-\nu^{(k)})\frac{d^2}{d\bar{x}_3^2}f^{(k)}_j(\bar{x}_3)\right]\quad j=1,\dots,4,$$

$$P^{(k)}_{33,jmn}(\bar{x}_3)=0$$

$$P^{(k)}_{13,jmn}(\bar{x}_3)=-q_{mn}\left(\frac{\pi nh}{b}\right)\exp\left[\gamma^{(k)}\left(\frac{x_3}{h}-1\right)\right]\frac{d}{d\bar{x}_3}f^{(k)}_j(\bar{x}_3)$$

$$P^{(k)}_{23,j}(\bar{x}_3)=q_{mn}\left(\frac{\pi mh}{a}\right)\exp[\gamma^{(k)}(\bar{x}_3-1)]\frac{d}{d\bar{x}_3}f^{(k)}_j(\bar{x}_3)$$

$$P^{(k)}_{11,jmn}(\bar{x}_3)=2q_{mn}\left(\frac{\pi nh}{b}\right)\left(\frac{\pi mh}{a}\right)\exp[\gamma^{(k)}(\bar{x}_3-1)]f^{(k)}_j(\bar{x}_3)$$

$$P^{(k)}_{22,jmn}(\bar{x}_3)=-2q_{mn}\left(\frac{\pi nh}{b}\right)\left(\frac{\pi mh}{a}\right)\exp[\gamma^{(k)}(\bar{x}_3-1)]f^{(k)}_j(\bar{x}_3)$$

$$P^{(k)}_{12,jmn}(\bar{x}_3)=q_{mn}\left[\left(\frac{\pi mh}{a}\right)^2-\left(\frac{\pi nh}{b}\right)^2\right]\exp[\gamma^{(k)}(\bar{x}_3-1)]f^{(k)}_j(\bar{x}_3)$$

$j=5,\ 6.$

In the expressions above, $\bar{x}_3=x_3/h$, and functions $f^{(k)}_j(\bar{x}_3)(j=1,\dots,6)$ are

$$f^{(k)}_1(\bar{x}_3)=\exp\left(\frac{\gamma^{(k)}\bar{x}_3}{2}\right)\cosh\lambda^{(k)}\bar{x}_3\cos\mu^{(k)}\bar{x}_3,$$

$$f^{(k)}_2(\bar{x}_3)=\exp\left(\frac{\gamma^{(k)}\bar{x}_3}{2}\right)\sinh\lambda^{(k)}\bar{x}_3\cos\mu^{(k)}\bar{x}_3,$$

$$f^{(k)}_3(\bar{x}_3)=\exp\left(\frac{\gamma^{(k)}\bar{x}_3}{2}\right)\cosh\lambda^{(k)}\bar{x}_3\sin\mu^{(k)}\bar{x}_3,$$

$$f^{(k)}_4(\bar{x}_3)=\exp\left(\frac{\gamma^{(k)}\bar{x}_3}{2}\right)\sinh\lambda^{(k)}\bar{x}_3\sin\mu^{(k)}\bar{x}_3,$$

$$f^{(k)}_5(\bar{x}_3)=\exp\left(-\frac{\gamma^{(k)}\bar{x}_3}{2}\right)\cosh\beta^{(k)}\bar{x}_3,$$

$$f^{(k)}_6(\bar{x}_3)=\exp\left(-\frac{\gamma^{(k)}\bar{x}_3}{2}\right)\sinh\beta^{(k)}\bar{x}_3.$$

References

Abrate, S., 1998. Impact on Composite Structures. Cambridge University Press, New York, NY, USA.

Alibeigloo, A., 2014. Three-dimensional thermo-elasticity solution of sandwich cylindrical panel with functionally graded core. Compos. Struct. 107, 458–468.

Alibeigloo, A., Liew, K.M., 2014. Free vibration analysis of sandwich cylindrical panel with functionally graded core using three-dimensional theory of elasticity. Compos. Struct. 113, 23–30.

Anderson, T.A., 2003. A 3-D elasticity solution for a sandwich composite with functionally graded core subjected to transverse loading by a rigid sphere. Compos. Struct. 60, 265–274.

Apetre, N.A., Sankar, B.V., Ambur, D.R., 2008. Analytical modeling of sandwich beams with functionally graded core. J. Sandwich Struct. Mater. 10, 53–74.

Bai, X.M., Guo, L.C., Wang, Z.H., Zhong, S.Y., 2013. A dynamic piecewise-exponential model for transient crack problems of functionally graded materials with arbitrary mechanical properties. Theoret. Appl. Fract. Mech. 66, 41–51.

Birman, V., Byrd, L.W., 2007. Modelling and analysis of functionally graded materials and structures. Appl. Mech. Rev. 60, 195–216.

Etemadi, E., Afaghi Khatibi, A., Takaffoli, M., 2009. 3D finite element simulation of sandwich panels with a functionally graded core subjected to low velocity impact. Compos. Struct. 89, 28–34.

Guo, L.C., Noda, N., 2007. Modeling method for a crack problem of functionally graded materials with arbitrary properties – piecewise-exponential model. Int. J. Solids Struct. 44, 6768–6790.
Icardi, U., Ferrero, L., 2009. Optimisation of sandwich panels with functionally graded core and faces. Compos. Sci. Technol. 69, 575–585.
Jha, D.K., Kant, T., Singh, R.K., 2013. A critical review of recent research on functionally graded plates. Compos. Struct. 96, 833–849.
Kashtalyan, M., 2004. Three-dimensional elasticity solution for bending of functionally graded rectangular plates. Eur. J. Mech. A Solids 23, 853–864.
Kashtalyan, M., Menshykova, M., 2009. Three-dimensional elasticity solution for sandwich panels with a functionally graded core. Compos. Struct. 87, 36–43.
Kirugulige, M.S., Kitey, R., Tippur, H.V., 2005. Dynamic fracture behaviour of model sandwich structures with functionally graded core: a feasibility study. Compos. Sci. Technol. 65, 1052–1068.
Liew, K.M., Zhao, X., Ferreira, A.J.M., 2011. A review of meshless methods for laminated and functionally graded plates and shells. Compos. Struct. 93, 2031–2041.
Liu, T.J., Xing, Y.M., 2014. Analysis of graded coatings for resistance to contact deformation and damage based on a new multi-layer model. Int. J. Mech. Sci. 81, 158–164.
Liu, X.R., Tian, X.G., Lu, T.J., Liang, B., 2014. Sandwich plates with functionally graded metallic foam cores subjected to air blast loading. Int. J. Mech. Sci. 84, 61–72.
Noda, N., 1999. Thermal stresses in functionally graded materials. J. Therm. Stresses 22, 477–512.
Ootao, Y., 2011. Transient thermoelastic analysis for a multilayered thick strip with piecewise exponential nonhomogeneity. Compos. B Eng. 42, 973–981.
Ootao, Y., Ishihara, M., 2013. Three-dimensional solution for transient thermoelastic problem of a functionally graded rectangular plate with piecewise exponential law. Compos. Struct. 106, 672–680.
Plevako, V.P., 1971. On the theory of elasticity of inhomogeneous media: PMM. vol. 35. n ≙ 5. 1971. pp. 853–860. J. Appl. Math. Mech. 35, 806–813.
Rahmani, O., Khalili, S.M.R., Malekzadeh, K., Hadavinia, H., 2009. Free vibration analysis of sandwich structures with a flexible functionally graded syntactic core. Compos. Struct. 91, 229–235.
Reddy, J.N., 2000. Analysis of functionally graded plates. Int. J. Numer. Methods Eng. 47, 663–684.
Sburlati, R., 2012. An axisymmetric elastic analysis for circular sandwich panels with functionally graded cores. Compos. B Eng. 43, 1039–1044.
Swaminathana, K., Naveenkumara, D.T., Zenkour, A.M., Carrera, E., 2015. Stress, vibration and buckling analyses of FGM plates—a state-of-the-art review. Compos. Struct. 120, 10–31.
Wang, E., Gardner, N., Shukla, A., 2009. The blast resistance of sandwich composites with stepwise graded cores. Int. J. Solids Struct. 46, 3492–3502.
Woodward, B., Kashtalyan, M., 2010. Bending response of sandwich panels with graded core: 3D elasticity analysis. Mech. Adv. Mater. Struct. 178, 586–594.
Woodward, B., Kashtalyan, M., 2011. 3D elasticity analysis of sandwich panels with graded core under distributed and concentrated loadings. Int. J. Mech. Sci. 53, 872–885.
Woodward, B., Kashtalyan, M., 2012. Finite element modelling of sandwich panels with graded core under various boundary conditions. Aeronaut. J. 1186, 1285–1310.
Xu, G., Zhai, J., Zeng, T., Wang, Z., Cheng, S., Fang, D., 2015. Response of composite sandwich beams with graded lattice core. Compos. Struct. 119, 666–676.
Zenkour, A.M., 2006. Generalized shear deformation theory for bending analysis of functionally graded plates. Appl. Math. Model. 30, 67–84.
Zhou, J., Guan, Z.W., Cantwell, W.J., 2013. The impact response of graded foam sandwich structures. Compos. Struct. 97, 370–377.
Zhu, H., Sankar, B.V., 2007. Analysis of sandwich TPS panel with functionally graded foam core by Galerkin method. Compos. Struct. 77, 280–287.